


Dual ionic crosslinked interpenetrating network of alginate-cellulose beads with enhanced mechanical properties for biocompatible encapsulation

Kangseok Lee · Jisu Hong · Hyun Ji Roh · Soo Hyun Kim ·
Hyunjung Lee · Sung Kuk Lee · Chaenyung Cha 

Received: 9 May 2017 / Accepted: 14 August 2017 / Published online: 19 August 2017
© Springer Science+Business Media B.V. 2017

Abstract Alginate beads have been a popular carrier of a wide array of biologically relevant molecules, such as proteins, genes, and cells, for biomedical applications. However, the difficulty of controlling their mechanical properties as well as maintaining the long-term structural integrity has prevented more widespread utilization. Herein, a simple yet highly efficient method of engineering alginate beads with improved mechanical properties is presented, whereby a secondary network of biocompatible anionic cellulose is created within

the alginate network. The aqueous-soluble anionic cellulose, containing either carboxylate or sulfonate, is found to undergo crosslinking reaction with trivalent ions more favorably than divalent ions, necessitating a dual sequential ionic crosslinking scheme to create interpenetrating networks (IPN) of alginate and cellulose with divalent and trivalent ions, respectively. The IPN alginate-cellulose beads demonstrate superior mechanical strength and controllable rigidity as well as enhanced resistance to harsh chemical environment as compared to alginate beads. Furthermore, their suitability for biomedical applications is also demonstrated by encapsulating microbial species to maximize their bioactivity and therapeutic agents for controlled release.

Electronic supplementary material The online version of this article (doi:[10.1007/s10570-017-1458-8](https://doi.org/10.1007/s10570-017-1458-8)) contains supplementary material, which is available to authorized users.

K. Lee · H. J. Roh · S. K. Lee · C. Cha
School of Life Sciences, Ulsan National Institute of
Science and Technology (UNIST), Ulsan 44919, Korea

J. Hong · C. Cha (✉)
School of Materials Science and Engineering, Ulsan
National Institute of Science and Technology (UNIST),
Ulsan 44919, Korea
e-mail: ccha@unist.ac.kr

S. H. Kim · H. Lee
School of Advanced Materials Engineering, Kookmin
University, Seoul 02707, Korea

S. K. Lee
School of Energy and Chemical Engineering, Ulsan
National Institute of Science and Technology (UNIST),
Ulsan 44919, Korea

Keywords Alginate · Anionic cellulose ·
Interpenetrating network · Dual ionic crosslinking ·
Hydrogel bead

Introduction

Spherical alginate hydrogels ('beads') have a place in modern history of biomedical engineering as one of the first and most widely utilized materials (Gombotz and Wee 2012; Hari et al. 1996; Lee and Mooney 2012; Tønnesen and Karlsen 2002). Alginate, a natural anionic polysaccharide with a carboxylic functional group on each saccharide unit, is capable of electrostatic interaction with multivalent cations to

form the crosslinked network. Their applications mainly lie in the area of drug and cell delivery, due to their highly attractive physical properties (e.g. elasticity, high water content) as well as biocompatibility, abundant raw material, tunable size (down to micron scale), mild reaction conditions, simple and efficient fabrication route (George and Abraham 2006; Hari et al. 1996; Lim and Sun 1980; Smidsrød 1990; Sugiura et al. 2005). The alginate beads have been successfully used to encapsulate a wide array of biologically relevant moieties, from therapeutic agents (e.g. small molecules, proteins, and genes) to living species (e.g. microbes, mammalian cells), with several efforts underway for clinical translation (Gombotz and Wee 2012; Lim and Sun 1980; Smidsrød 1990; Tønnesen and Karlsen 2002). They have been shown to provide fast and yet safe encapsulating environment which significantly enhances the initial loading efficiency, whereas most other methods utilize more elaborate chemical reactions that often involve harsh conditions, causing the damage of encapsulating entities. In addition, the diffusive nature of alginate hydrogels allows for the release of encapsulated agents and perfusion of media for long-term cell culture, while circumventing the infiltration of immune cells.

An attractive and yet often overlooked aspect of engineering alginate beads is the ability for safe and efficient mass production, which is an important prerequisite for large-scale industrial applications. This is due to the characteristic ionic crosslinking scheme, in which the alginate beads are almost instantaneously formed by placing alginate solution droplets into a bath containing crosslinking ions. For example, alginate beads are used as immobilizing capsules for engineered microbes for industrial “green biotechnology”, such as biofuel production and environmental clean-up (Covarrubias et al. 2012; Rathore et al. 2013). The alginate beads have been shown to prolong the biological activity of the encapsulated microbes with mechanical support, aqueous microenvironment, and protection against harsh external surroundings. The beads are also used as carriers for the sustained release of inoculants and herbicides for farming (Bashan 1986; Pfister et al. 1986).

Despite these favorable attributes and a relatively long history of research and development, the utilization of alginate beads has not met with more

widespread commercial success, largely due to the lack of long term stability. The ionic crosslinking that allows for the efficient fabrication of alginate beads ironically has been a deterrent, because the ions leach out over time leading to premature mechanical failure and structural disintegration, often facilitated by the presence of chemicals capable of chelation or ion exchange Thu et al. (1996a, b). Unlike the controlled laboratory settings, large-scale industrial processes often contain many chemical additives that cause the ion leaching. In addition, it is difficult to control the mechanical properties of the beads because the range of alginate concentration is extremely limited, usually less than 2% (w/v), due to its high viscosity. For these reasons, several strategies have been introduced to enhance the mechanical properties of the beads, such as hybridization with other polymeric networks and nanocomposite formation (Fan et al. 2013; Kulkarni et al. 2001; Shi et al. 2008; Zhang et al. 2010). However, these methods involve the use of harsh chemicals that may have deleterious effects on the encapsulated species. In addition, they generally involve several additional processing steps, losing the appeal of efficient mass production of the alginate beads. Therefore, developing a strategy of enhancing and controlling the mechanical performance of the alginate beads, while maintaining the biocompatibility and efficient processability, is crucial to further improve their quality for broader applicability.

In this study, a simple yet highly effective strategy of enhancing the structural and mechanical properties of alginate beads is presented, in which an interpenetrating network (IPN) consisting of anionic cellulose is created within the alginate bead via ionic crosslinking. Cellulose, a natural polysaccharide commonly found in plants as a fibrous structural element, is the most abundant natural polymer, and has a wide range of industrial uses (Kil and Paik 2015; Ko et al. 2015). Given its obvious biocompatibility along with the natural fibrous morphology, it has also found its way into biomedicine, most notably as wound dressing and engineered tissue scaffolds (Hoenich 2006; Jorfi and Foster 2015; Sindhu et al. 2014). Since the natural cellulose is insoluble, various forms of aqueous-soluble cellulose have also been developed and widely used as additives in medical and pharmaceutical applications (Hoenich 2006; Jorfi and Foster 2015; Lee et al. 2016; Shen et al. 2016; Sindhu et al. 2014; Siritientong and Aramwit 2015; Xiong et al. 2015;

Zhang 2001). Herein, two different types of anionic cellulose, carboxymethyl cellulose (CMC) and sulfoethyl cellulose (SEC), were chosen as secondary polymeric networks to the primary alginate network. CMC has been shown to undergo ionic crosslinking with trivalent ions such as Al^{3+} (Chitprasert et al. 2012; Siritientong and Aramwit 2015). Therefore, a sequential ionic crosslinking scheme was employed to first develop the bead structure by crosslinking alginate with divalent Ca^{2+} , followed by crosslinking anionic cellulose with Al^{3+} . It was hypothesized that this dual crosslinked IPN alginate-cellulose beads would provide a facile and effective route of generating hydrogel beads with tunable mechanical properties and enhanced structural durability. In addition, with this improved mechanical functionalities, the IPN alginate-cellulose beads would also allow for controlling the release kinetics of encapsulated drug molecules and promote the survival and biological activity of encapsulated cells.

Materials and methods

Synthesis of anionic cellulose

The conjugation of aqueous-soluble anionic functional groups onto cellulose was accomplished via etherification of hydroxyl groups of cellulose, following previous published reports with modifications (Ramos et al. 2005). To synthesize carboxymethyl cellulose (CMC), cellulose (1 g, Sigma Aldrich) was first dissolved in dimethyl sulfoxide (30 mL) supplemented with tetrabutylammonium fluoride (9 wt%) at 60 °C. Sodium hydroxide powder (3.7 g, Sigma Aldrich) was dispersed into the reaction mixture and continuously stirred for 2 h at room temperature for mercerization. Sodium chloroacetate (7.2 g, Sigma Aldrich) was slowly added to the mixture and continuously stirred for 24 h at 60 °C. The entire procedure was performed under dry N_2 gas. The mixture was neutralized with acetic acid (10%) and precipitated in excess diethyl ether to obtain the crude product. Then, it was dialyzed against deionized (DI) water, and then lyophilized to obtain the final product. The conjugation of carboxymethyl groups onto cellulose was determined with FT-IR spectroscopy (Fig. S1 in Supplementary Information) and 1H -NMR (Fig. S2 in Supplementary Information).

The synthesis and characterization of sulfoethyl cellulose (SEC) were done following the same procedure as CMC (Fig. S1 in Supplementary Information) (Zhang et al. 2011). For SEC, sodium bromoethanesulfonate (Alfa Aesar) was used as the reactant to conjugate sulfonate groups onto cellulose.

Fabrication of alginate-cellulose IPN beads

High molecular weight sodium alginate (220,000 $g\ mol^{-1}$, Junsei Chemical, Japan) and CMC were dissolved in DI water at 2% separately as stock solutions. Alginate and CMC solutions were mixed in a varying ratio to develop a working precursor solution, which was then added to a syringe connected to an 18G needle (BD Biosciences). Using an electronic syringe pump (Legato 100, KD Scientific), the solution was extruded out slowly and the droplets being formed were immediately placed into a bath of 0.1 M calcium chloride solution. The beads were left in the bath for 1 h for complete crosslinking, and then kept in DI water for further characterization.

To induce IPN of anionic cellulose within the alginate bead, the beads were transferred to a bath of aluminum chloride solution and incubated for 1 h. Iron(III) chloride and chromium(III) chloride solutions were also used in place of aluminum chloride. These same experiments were performed using SEC as a secondary network.

Functional characterizations of alginate-cellulose IPN beads

Mechanical properties

Mechanical properties of various hydrogel beads were evaluated from force–displacement relationships obtained from compression experiments. Briefly, each bead was compressed at the rate of $1\ mm\ min^{-1}$ using a universal testing machine (Model 3343, Instron), and the force–displacement curve was obtained. The elastic modulus (E) was calculated using Hertz contact mechanics theory,

$$E = \frac{3F}{4} R^{-1/2} h^{-3/2} (1 - \nu^2) \quad (1)$$

where R was the radius of the bead, h was the displacement, and ν was the Poisson's ratio of the

bead which was set as 0.5, assuming the bead follows the ideal rubber (Cha et al. 2014; Hashmi and Dufresne 2009; Lin et al. 2007). Since this model works well at smaller displacements, the moduli of each bead were calculated within the range of strain from 0.05 to 0.15 and their average value was reported.

Structural durability of the IPN beads against harsh chemical environment was assessed with chelating agents (Cha et al. 2012). The beads were incubated in 20 mM ethylenediaminetetraacetic acid (EDTA, Sigma Aldrich) under constant shaking at 50 rpm, and the time required to completely dissolve the bead was measured. For each condition, ten beads were tested and their average and standard deviation values were reported.

The swelling ratio of a bead was calculated as the mass ratio of a swollen hydrogel (W_S) to its dried polymeric mesh (W_D). W_S was measured after incubating the bead in DI water for 24 h at 30 °C, and W_D was measured after drying the bead by lyophilization.

Drug release

Bovine serum albumin ('BSA', Sigma Aldrich) was encapsulated into the beads, and the release was recorded over time. Briefly, BSA (2 mg mL⁻¹) was dissolved in a precursor solution prior to fabrication. The gel beads were fabricated via ionic crosslinking as mentioned above. Each bead was incubated in 0.2 mL of PBS at 37 °C. At each various times up to 48 h, the medium was collected and the BSA concentration was measured using BCATM Protein Assay (Thermo Fisher), following the manufacturer's instructions. For the release profiles with a power-law dependence on time, they were fitted using the Ritger–Peppas equation,

$$\frac{M_t}{M_\infty} = k \cdot t^n \quad (2)$$

where M_t is the cumulative amount of drug released at a time, t ; M_∞ is the total amount of drug in the microspheres; k is the kinetic rate constant; and n is the exponent related to the release mechanism (Kim et al. 2016; Serra et al. 2006). For the release profiles

with sigmoidal dependence on time, they were fitted using the Weibull equation,

$$\frac{M_t}{M_\infty} = 1 - e^{-k(t-T)^b} \quad (3)$$

where k is the kinetic rate constant, T is the lag time constant, and b is the exponent related to the release mechanism (Dash et al. 2010).

Microbial bioactivity

Escherichia coli (*E. coli*) expressing enhanced green fluorescent protein (GFP⁺) was constructed by transforming *E. coli* strain, BL21(DE3), with a plasmid containing the gene encoding GFP⁺ (*gfp*⁺). Here, GFP⁺ was a genetic variant of the wild-type GFP with two mutations, S65T and F64L, well known to express higher fluorescence than the wild-type GFP (Cormack et al. 1996). The plasmid was constructed by replacing the RFP-encoding gene (*rfp*) of pBbE7 K-*rfp* (plasmid #35315, <http://www.addgene.org>) with *gfp*⁺, to give pBbE7 K-*gfp*⁺ (Lee et al. 2011). The reconstructed GFP⁺-expressing *E. coli* was cultured in Luria broth (LB) medium at 30 °C with shaking (200 rpm) until the OD₆₀₀ became 1.8. Then, 1 mL of the cell mixture was taken and the cells were isolated by centrifugation (5000 rpm, 5 min). The cell pellet was carefully suspended in 1 mL of bead precursor solution via gentle pipetting, followed by bead fabrication as described above. The cell-encapsulated beads were first washed in DI water, and then incubated in LB medium at 30 °C with shaking (100 rpm).

The viability of cells encapsulated in the beads was evaluated with MTT assay (Cha et al. 2012; Jang et al. 2017). Briefly, a bead was placed in a well of a 96-well plate with 100 μL of LB medium containing 0.5 mg mL⁻¹ of MTT solution (3-(4,5-dimethylthiazol-2-yl)-2,5-diphenyltetrazolium bromide (MTT, Sigma Aldrich)) and incubated for 4 h at 30 °C. Then, 100 μL of the stop solution [20% sodium dodecyl sulfate in water/dimethylformamide (50:50)] was added and further incubated for 4 h with shaking (100 rpm) at room temperature to dissolve the MTT formazan formed by the living cells. The medium was collected and its absorbance at 570 nm was measured using a UV/Vis spectrometer (Multiskan GO, Thermo Fisher).

The GFP expression from the encapsulated cells was evaluated by measuring the fluorescence intensity. Each bead was placed in a well of 384-well plate, and the fluorescence emission from the bead was measured at various times using a spectrofluorometer (Synergy HTX, BioTek).

Results and discussion

Fabrication of alginate-cellulose IPN beads

Cellulose has been one of the most extensively used materials for biomedical applications, from medical products (e.g. wound dressing and membranes) to food and drug additives. There are also significant research efforts to utilize cellulose for other research areas, such as drug delivery and tissue engineering. The natural cellulose exists in fibrous forms; therefore it is often modified to present functional groups for aqueous solubility which allows for more diverse applications. Carboxymethyl cellulose (CMC) is among the earliest and most widely investigated aqueous-soluble cellulose for its high solubility at wide ranges of temperature and concentration, owing to the carboxylic salt form (Ramos et al. 2005; Zhang 2001). The negatively charged carboxylic groups of CMC also allows for tuning material properties such as viscosity and the interaction with biological molecules for controlled delivery applications (Yang and Zhu 2007).

Another unique property of CMC is the ability to undergo ionic interaction with multivalent ions. In particular, CMC molecules have been shown to be readily crosslinked by trivalent ions such as Al^{3+} and Fe^{3+} (Emregül et al. 1996; Fang and Cathala 2011; Xiao et al. 2009). Inspired by this capability, it was hypothesized that introducing the ionically crosslinked network of CMC within alginate beads would significantly enhance their mechanical properties. There have been several studies demonstrating hybrid networks of alginate and aqueous-soluble cellulose such as CMC, but they were fabricated together with the same ionic crosslinker (Agarwal et al. 2015; Kim et al. 2012). However, since alginate and cellulose have different reactivities towards divalent and trivalent ions, alginate and CMC were sequentially crosslinked using divalent and trivalent ions, respectively, to engineer interpenetrating network (IPN) beads of alginate and CMC in this study (Fig. 1a). With this

approach, it was further postulated that controlling the mechanical properties of the beads at wider ranges could be made possible by separately controlling the crosslinking densities of alginate and CMC.

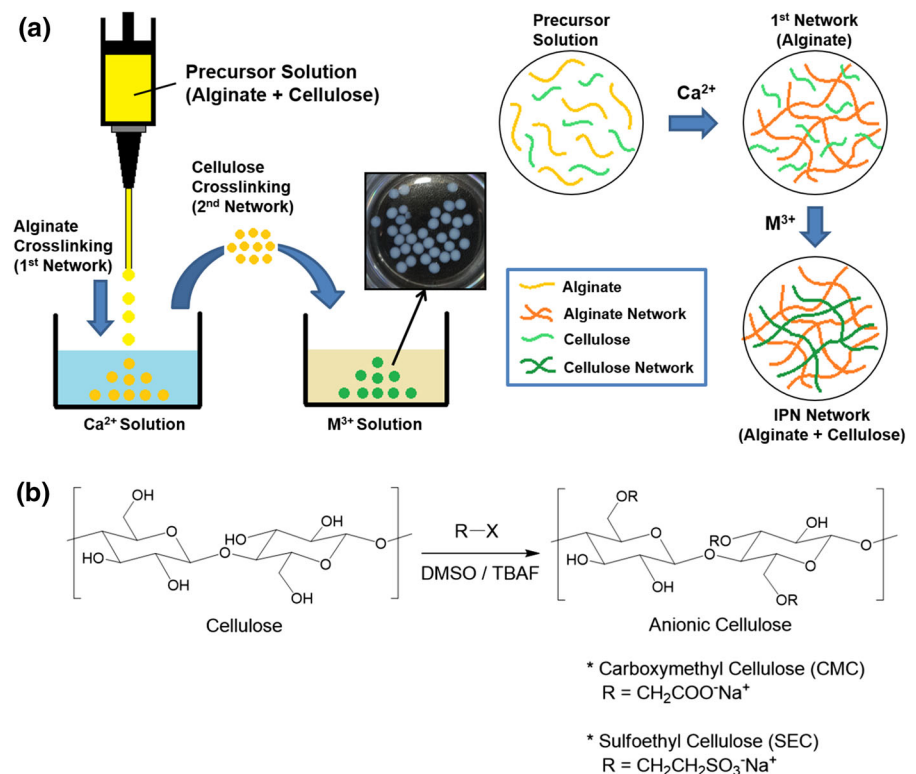
CMC was synthesized by etherification of hydroxyl groups of cellulose by sodium chloroacetate (Fig. 1b). To compare and vary the degree of ionic crosslinking of cellulose, another type of anionic cellulose containing sulfonate groups, namely sulfoethyl cellulose (SEC), was also synthesized and used to fabricate the IPN beads. Due to the difference in ionic strength between carboxylate and sulfonate in aqueous environment, there would be a difference in the degree of ionic crosslinking, and as a result, a difference in the mechanical properties of the IPN beads. The primary network was first developed by placing droplets of a precursor solution containing 1% alginate and a varying concentration of CMC up to 1% into a calcium chloride solution (0.1 M), which resulted in immediate bead formations, as expected. The beads were then transferred to an aluminum chloride solution (0.1 M) to further crosslink the CMC within the beads to fabricate the IPN alginate-CMC beads. Compared to the Ca^{2+} -crosslinked beads ('Ca-alginate-CMC beads'), the IPN beads became more opaque, suggesting there was a further crosslinking reaction by Al^{3+} (Fig. 2a, Fig. S3 in Supplementary Information). The IPN alginate-SEC beads were also developed following the same procedure as the IPN alginate-CMC beads. There was also increase in opacity, but it was not as noticeable as the IPN alginate-CMC beads.

Mechanical properties of IPN alginate-cellulose beads

Effect of IPN formation by Al^{3+} on rigidity

The elastic moduli of various beads were measured to evaluate their mechanical properties in response to different crosslinking conditions. There was a small increase in the moduli of Ca-alginate-CMC beads with increasing CMC concentration up to 0.5% (1.8-fold increase), but further increase in CMC concentration to 1% did not enhance the modulus (Fig. 2b). This result suggests the CMC within the alginate bead could participate in the ionic crosslinking reaction with Ca^{2+} to a certain degree. When these beads were further crosslinked with Al^{3+} to generate IPN alginate-CMC beads, however, there was a much greater

Fig. 1 **a** Schematic representation of the alginate-cellulose IPN bead fabrication via dual ionic crosslinking. **b** Synthesis of anionic cellulose via etherification



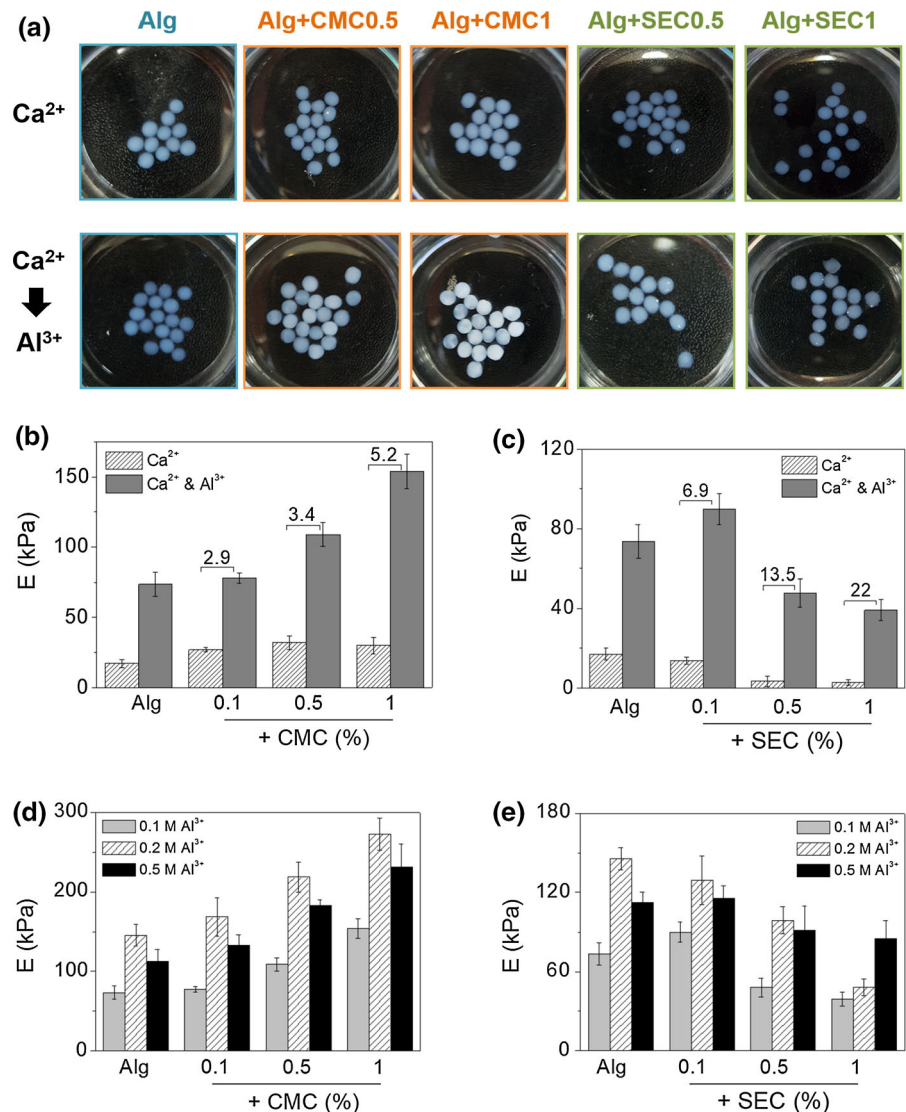
increase in the moduli for all condition compared to the Ca-alginate-CMC beads, and the increase was proportional to the CMC concentration (e.g. 2.9-fold increase for 0.1% CMC, 3.4-fold increase for 0.5% CMC, 5.2-fold increase for 1% CMC), demonstrating the preferential crosslinking of CMC by Al³⁺.

It is interesting to note that the alginate beads without CMC also showed increase in modulus by further crosslinking Al³⁺, though it was not as significant as those with CMC. This result indicated that Al³⁺ could also crosslink alginate molecules. In order to further evaluate the nature of crosslinking of alginate by Al³⁺ by comparing the crosslinking efficiency with Ca²⁺, a control experiment was performed in which the droplets of alginate precursor solution were placed into Al³⁺ solution. Interestingly, the resulting beads were not formed properly; they were structurally weak, eventually disintegrated over time, and their shape was more flat (disk-shaped) likely due to the impact when the droplets hit the Al³⁺ solution (Fig. S4 in Supplementary Information). This result clearly demonstrated that the alginate bead formation was much more efficient with Ca²⁺ than Al³⁺ even though the positive charge was lower.

Since aluminum ions are known to form complex species with water molecules and hydroxide ions as ligands (e.g. Al(H₂O)₆³⁺, Al(OH)₂²⁺, Al(OH)₂⁺), it was thus suggested that more time was required for alginate to replace the ligands and interact with Al³⁺ as compared to Ca²⁺ which already existed in the fully ionized form and readily interacted with alginate (Van Benschoten and Edzwald 1990). This result further indicated that only after the alginate molecules were immobilized by Ca²⁺, did Al³⁺ diffuse into the alginate beads interact with the remaining negatively charged carboxylic groups.

The alginate-SEC beads were prepared in the same manner and their moduli were measured. The moduli of Ca-alginate-SEC beads, unlike CMC, gradually decreased with increasing SEC concentration (Fig. 2c). This result indicated that Ca²⁺ crosslinking of alginate was hindered by the presence of SEC, rather than participating in the crosslinking and contributing to enhancing the overall mechanical properties. Sulfonate is generally a weaker base than carboxylate, it is thus suggested that the sulfonate groups in SEC could not efficiently interact with Ca²⁺ compared to the carboxylate groups of CMC. When

Fig. 2 **a** Photographs of alginate beads, alginate-CMC beads, and alginate-SEC beads crosslinked by Ca^{2+} or Ca^{2+} followed by 0.1 M Al^{3+} (IPN). Elastic moduli (E) of **b** alginate-CMC beads and **c** alginate-SEC beads with varying CMC or SEC concentrations, crosslinked by Ca^{2+} or IPN. The number shown on the graphs represents the fold increase by the IPN formation for each condition. E values of **d** IPN alginate-CMC beads and **e** IPN alginate-SEC beads crosslinked by varying concentrations of Al^{3+} (0.1, 0.2, and 0.5 M)



they were further crosslinked with Al^{3+} to generate IPN alginate-SEC beads, the moduli increased significantly with increasing SEC concentration, as compared to the Ca-alginate-SEC beads (e.g. 6.9-fold increase for 0.1% SEC, 13.5-fold increase for 0.5% SEC and 22-fold for 1% SEC), which was similarly shown for the IPN alginate-CMC beads (Fig. 2c). These results highlight the preferential crosslinking of anionic cellulose by trivalent ions over divalent ions. Furthermore, it is interesting to note that although the overall moduli were higher for IPN alginate-CMC beads, the increase in moduli by Al^{3+} crosslinking was greater for IPN alginate-SEC

beads, likely due to the greater number of available sulfonate groups for crosslinking by Al^{3+} compared to carboxylic groups of CMC, as CMC was shown to participate in the crosslinking by Ca^{2+} more so than SEC.

Effect of Al^{3+} concentration on rigidity

The concentration of Al^{3+} was varied to control the degree of secondary crosslinking density of the anionic cellulose. For IPN alginate-CMC beads, increasing Al^{3+} concentration from 0.1 to 0.2 M resulted in higher moduli at all conditions (Fig. 2d).

However, there was a small decrease in moduli when Al^{3+} concentration was increased up to 0.5 M, indicating the CMC within the beads have fully participated in the crosslinking reaction, and excess Al^{3+} disrupted the existing ionic crosslinks.

For IPN alginate-SEC beads, there was a similar trend of moduli with increasing Al^{3+} concentration (Fig. 2e). However, unlike IPN alginate-CMC beads whose moduli decreased at all conditions at 0.5 M Al^{3+} , the moduli continued to increase with SEC concentration at 0.5 M Al^{3+} , suggesting there was a sufficient number of free sulfonate groups still available for crosslinking even at a higher Al^{3+} concentration. This result further corroborated the previous assertion that there was greater availability of sulfonate groups for further crosslinking by Al^{3+} , as SEC did not participate in the initial crosslinking of alginate by Ca^{2+} as much as CMC. Taken together, controlling the crosslinking density of a secondary cellulose network with Al^{3+} allowed for enhancing the mechanical properties of the IPN beads.

Effect of non-anionic functional groups of cellulose on IPN formation

To further validate the IPN network formation of alginate and anionic cellulose via dual ionic crosslinking, non-anionic celluloses were also used to generate the IPN beads. Here, methyl cellulose (MC), hydroxyethyl cellulose (HEC), and cellulose trimethylammonium chloride (CTMAC) were chosen, as they possess functional groups that do not form electrostatic interactions with cationic species. For HEC, the moduli of Ca-alginate-HEC beads decreased with HEC concentration up to 0.5% (from 17 to 9 kPa), but increased at 1% HEC (15.5 kPa) (Fig. S5a in Supplementary Information). HEC without the ability for ionic crosslinking likely hindered crosslinking between alginate and Ca^{2+} , but at higher concentration, HEC may have acted as a filler in the alginate-HEC beads leading to increased moduli. The moduli of IPN alginate-HEC beads were smaller than that of alginate beads at all conditions, demonstrating that there was negligible, if at all, secondary crosslinking by Al^{3+} .

On the other hand with MC, the moduli of Ca-alginate-MC beads increased with MC concentration up to 0.5% (from 17 to 27 kPa), but decreased at 1%

MC (16 kPa) (Fig. S5b in Supplementary Information). The methyl groups likely underwent hydrophobic interaction among MC molecules, but further increase in local hydrophobicity may have disrupted the ionic crosslinking. Like alginate-HEC beads, the moduli of IPN alginate-MC beads were either smaller than (below 0.5% MC) or similar to (at 1% MC) that of alginate beads, which also indicated the minimal role of secondary crosslinking by Al^{3+} .

Incorporating CTMAC, an aqueous-soluble cellulose with positively charged trimethylammonium chloride groups, into the alginate beads had a different effect on the rigidity. The moduli of Ca-alginate-CTMAC beads increased with CTMAC concentration up to 1% CTMAC, from 17 to 30 kPa. Ca^{2+} and CTMAC may have both contributed to the crosslinking of alginate, leading to increased moduli (Fig. S5c in Supplementary Information). However, the moduli of IPN alginate-CTMAC beads were much lower than those of IPN alginate-HEC beads and IPN alginate-MC beads, such that the moduli became similar to those of Ca-alginate-CTMAC beads at 0.5 and 1% CTMAC. This interesting result may have stemmed from Al^{3+} competing with and replacing CTMAC molecules that had already formed ionic interaction with alginate. Taken together, the aqueous-soluble celluloses without anionic functional groups were not able to form secondary network via ionic crosslinking with Al^{3+} , thereby proving the IPN formation of alginate-CMC and alginate-SEC beads by dual ionic crosslinking.

Swelling properties of IPN alginate-cellulose beads

Effect of IPN formation by Al^{3+} on swelling

In order for the IPN alginate-cellulose beads to be successfully utilized as a carrier of biological entities such as drug molecules and cells, it is imperative that the diffusivity of the beads must be sufficient enough to allow various drugs to be released at desired rates and provide nutritional support for the encapsulated cells. Therefore, the swelling ratios of the alginate-cellulose IPN beads were measured to evaluate the effect of various dual crosslinking conditions on the diffusional properties of the beads. According to the rubber-elasticity theory, the crosslinking density has

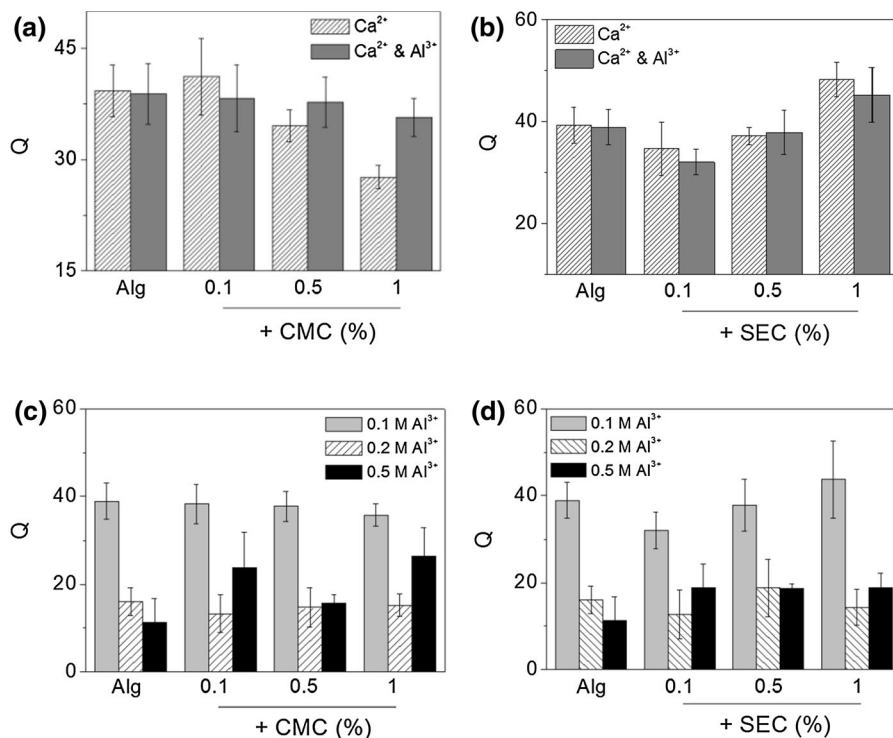
an opposite effect on the mechanical and diffusional properties of a material; increasing the crosslinking density, while enhancing the mechanical properties, usually decreases the diffusional properties as more crosslinked network prevents the entry of the surrounding fluids (Anseth et al. 1996). Since the dual ionic crosslinking was employed to control the varying degrees of crosslinking density of the IPN beads, this could inevitably lead to altered diffusional properties.

The swelling ratios of Ca-alginate-CMC beads gradually decreased with increasing CMC concentration, up to 45% at the highest CMC concentration of 1%, as compared to Ca-alginate beads (Fig. 3a). This result indicated that the CMC was able to participate in the extensive crosslinking reaction with the alginate by Ca^{2+} . On the other hand, the swelling ratios of IPN alginate-CMC beads did not decrease significantly with increasing CMC, only 14% decrease at 1% CMC, which is especially surprising considering that the rigidity of IPN alginate-CMC beads was much greater than that of Ca-alginate-CMC beads. This result may stem from the different nature chemical crosslinking by Al^{3+} from Ca^{2+} . The

mechanical properties of IPN alginate-CMC beads shown in Fig. 2 suggested that the polymeric network formed by Al^{3+} had greater impact on improving the mechanical properties of the existing network, but could not efficiently crosslink the polymers in a solution state as shown in Fig. S4. This suggested that trivalent Al^{3+} undergoes ionic crosslinking with more polymer chains at closer range than divalent Ca^{2+} , resulting in more space between crosslinks leading to higher degree of swelling. Furthermore, Chremos et al. have recently demonstrated that the higher-valent ions interacting with polyelectrolytes increase the local counter-ion concentration (Chremos and Douglas 2016). Thus it is possible that there was a greater ionic strength within the beads crosslinked by Al^{3+} than Ca^{2+} due to higher concentrations of counter-ions around the polymeric network, leading to increased hydrophilicity.

Similarly, the swelling ratios of Ca-alginate-SEC beads and IPN alginate-SEC beads were similar regardless of the SEC concentrations (Fig. 3b). Unlike alginate-CMC beads, there was a gradual increase in swelling with SEC concentration. Coupled with the decrease in moduli shown in Fig. 2c,

Fig. 3 Swelling ratios (Q) of **a** alginate-CMC beads and **b** alginate-SEC beads with varying CMC or SEC concentrations, crosslinked by Ca^{2+} or Ca^{2+} followed by 0.1 M Al^{3+} . Q values of **c** IPN alginate-CMC beads and **d** IPN alginate-SEC beads crosslinked by varying concentrations of Al^{3+} (0.1, 0.2, and 0.5 M)



alginate-SEC beads had lower crosslinking density than alginate-CMC beads, therefore confirming the presence of SEC within the alginate prevented efficient and extensive crosslinking by Ca^{2+} .

Effect of Al^{3+} concentration on swelling

The swelling ratios of IPN beads prepared by varying concentrations of Al^{3+} was also measured to evaluate the effect of crosslinking density of the cellulose network on the swelling properties of the resulting beads. As expected, increasing the Al^{3+} concentration from 0.1 to 0.2 M resulted in substantial decrease in swelling ratios for both IPN alginate-CMC and IPN alginate-SEC beads (Fig. 3c, d). Further increase in Al^{3+} concentration to 0.5 M did not significantly affect the swelling ratios of the resulting IPN beads. These results were in close accordance with the rigidity of the beads shown in Fig. 2d, e, demonstrating the expected inverse relationship.

Structural durability against chelating environment

Hydrogel beads prepared via ionic crosslinking are especially susceptible towards dissolution compared to covalent crosslinked hydrogels. The dissolution is often expedited by the presence of chelating chemicals in an aqueous environment that can induce the ion leaching from the beads Thu et al. (1996a, b). Unlike well-controlled laboratory settings, many biological and industrial applications involve the chemicals (e.g. citrate, phosphate, metalloenzymes, ethylenediaminetetraacetic acid (EDTA)) that can weaken the bead structures by chelation. Therefore,

the effect of dual ionic crosslinking of IPN beads on the structural durability against chelating agents was explored.

The alginate-cellulose IPN beads were incubated in a buffered solution containing EDTA, a well-known chelating agents used in biochemical applications, and the time required for complete disintegration of the bead structure was measured (Fig. 4). For IPN alginate-CMC beads, increasing CMC concentration from 0.1 to 1% resulted in delayed dissolution time, which was maximized when the Al^{3+} concentration was increased to 0.5 M (e.g. 270% increase in dissolution time from 0.1 to 1% CMC at 0.5 M Al^{3+} , Fig. 4a). Increased crosslinking density of the CMC network likely delayed the diffusion of EDTA into the beads. IPN alginate-SEC beads similarly displayed the delayed dissolution with increasing SEC concentration (e.g. 32% increase in dissolution time from 0.1 to 1% SEC at 0.1 M Al^{3+}) (Fig. 4b). However, unlike alginate-CMC beads, increasing Al^{3+} concentration did not have much effect on the dissolution time, likely due to the diminished crosslinking density as compared to IPN alginate-CMC beads.

Effect of different trivalent ions on IPN formation

In order to evaluate the role of trivalent ions on the IPN formation, other trivalent ions, Fe^{3+} and Cr^{3+} , were used to fabricate the IPN alginate-cellulose beads and their mechanical properties were measured and compared with those made with Al^{3+} (Emregül et al. 1996; Xiao et al. 2009). Their concentrations were also varied from 0.1 to 0.5 M. With the increase in concentration, the color of the beads became

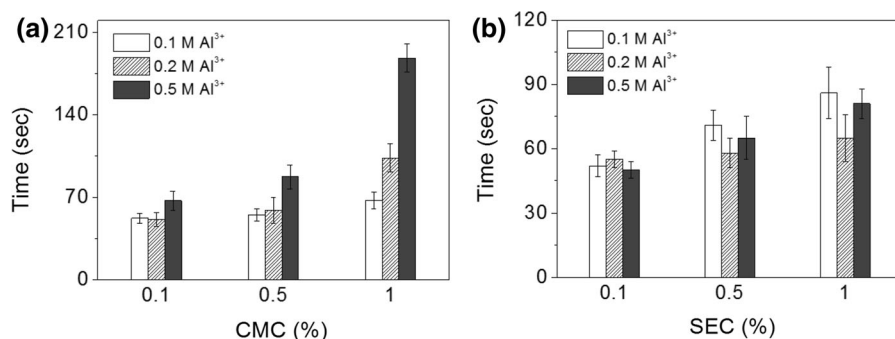


Fig. 4 Structural durability of **a** IPN alginate-CMC beads and **b** IPN alginate-SEC beads crosslinked by varying concentrations of Al^{3+} (0.1, 0.2, and 0.5 M), assessed by the time to completely dissolve the beads incubated in a chelating solution

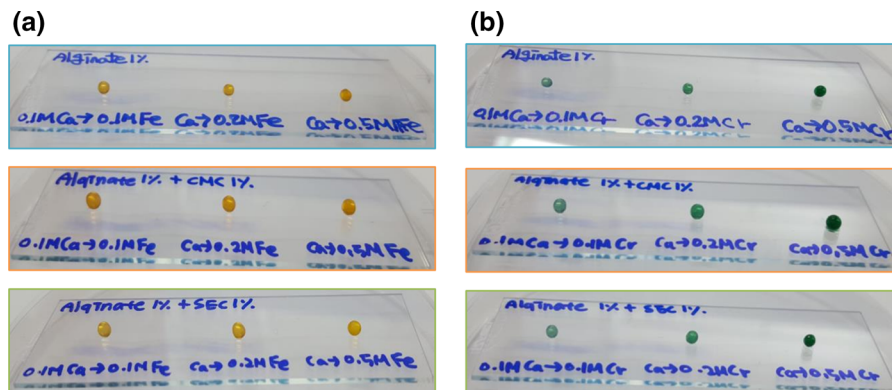


Fig. 5 Photographs of alginate beads, IPN alginate-CMC beads, and IPN alginate-SEC beads crosslinked by varying concentrations of **a** Fe^{3+} or **b** Cr^{3+}

stronger due to the increased presence of Fe^{3+} (yellow) and Cr^{3+} (green) (Fig. 5). The largest increase in moduli was attained using Fe^{3+} at all concentrations for both IPN alginate-CMC and alginate-SEC beads. Since Fe^{3+} is the heaviest and largest of the three ions (*i.e.* atomic numbers of Al, Cr, and Fe are 13, 24, and 26, respectively), it was likely able to interact more favorably with anionic functional groups (Fig. 6a, b). The effect of mass and size of crosslinking ions on the mechanical properties has been similarly demonstrated with alginate beads, in which the alginate beads crosslinked by larger and heavier divalent ions such as Ba^{2+} , Sr^{2+} , and Cd^{2+} were stronger than those crosslinked by Ca^{2+} (Mørch et al. 2006; Ouwerx et al. 1998).

However, at higher ion concentrations, the moduli of the Al^{3+} crosslinked beads became significantly larger than those of Cr^{3+} crosslinked beads at all CMC and SEC concentrations (Fig. 6c, d, e, f). It was suggested that the diffusivity of the ions through the beads may have played a greater role; smaller Al^{3+} was able to diffuse into the beads better than Cr^{3+} . It should be noted that regardless of the type of trivalent ions, the moduli of IPN alginate-CMC beads were generally larger than those of IPN alginate-SEC beads at higher cellulose concentrations.

As similarly done with Al^{3+} , the droplets of the bead precursor solution were placed into Cr^{3+} or Fe^{3+} solution, rather than Ca^{2+} , to generate the bead structures to compare the crosslinking efficiency (Fig. S6 in Supplementary Information). The beads made with Cr^{3+} were weak and did not form properly, which was similar with the Al^{3+} -

crosslinked beads. On the other hand, the beads made with Fe^{3+} were more mechanically robust, and their spherical shape was well maintained, although their rigidity was still much lower than those crosslinked with Ca^{2+} , which further highlighted the greater crosslinking efficiency of Fe^{3+} over Cr^{3+} . Regardless of the type of trivalent ions, the alginate crosslinking was much more efficient with divalent Ca^{2+} than the trivalent ions.

Drug release from IPN alginate-cellulose beads

The results of this study have demonstrated that the mechanical and swelling properties of the IPN alginate-cellulose beads could be controlled in a wide range by the concentration and crosslinking density of the cellulose network. Therefore, based on these results, it was hypothesized that these beads could be utilized as a controlled drug delivery system. To demonstrate, drug release profiles from various IPN alginate-cellulose beads were obtained and the release kinetics were analyzed. Here, bovine serum albumin (BSA) was chosen as a model protein drug.

For IPN alginate-CMC beads, the release profile followed a sigmoidal pattern, showing the initial delay before more extensive release (Fig. 7a). This type of release kinetics is commonly found in IPN networks where chain relaxations of both primary and secondary networks are required for more extensive drug release (Fu and Kao 2009). Therefore, these profiles were fitted with the Weibull model which accounts for the sigmoidal release pattern (Dash et al. 2010). The exponent value which represents the

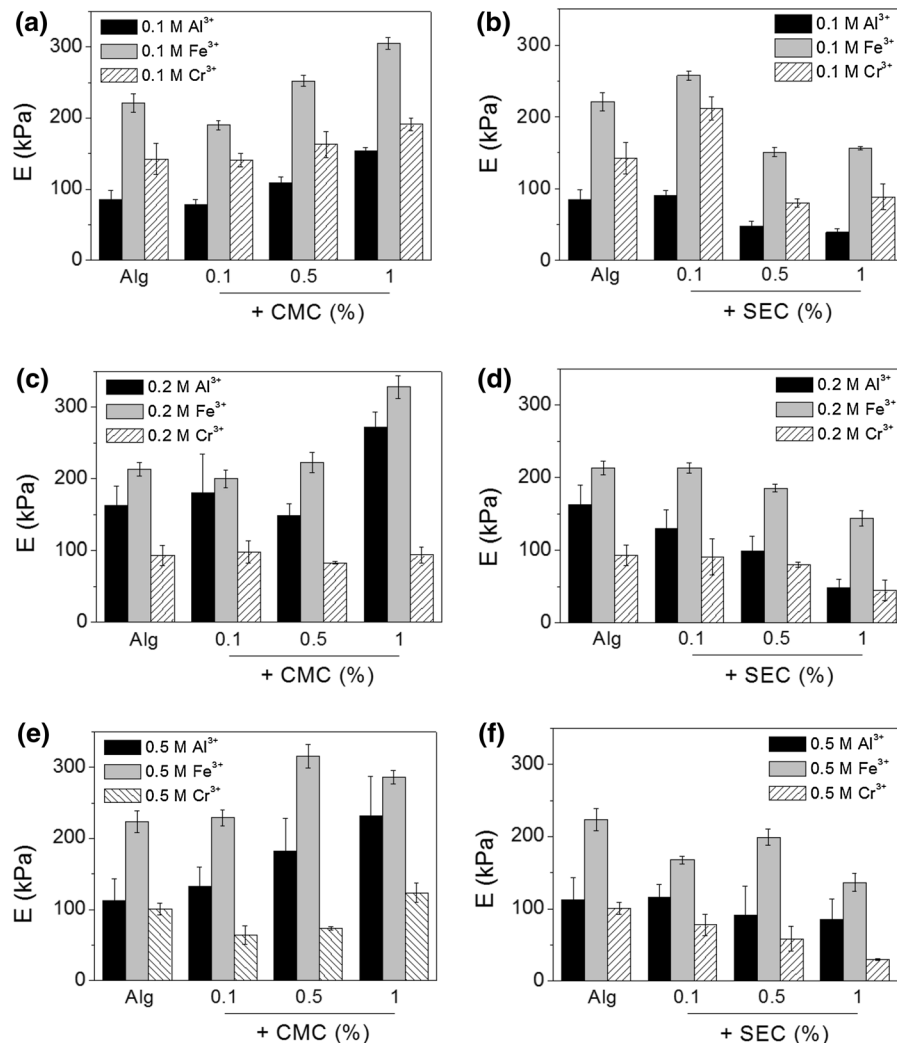


Fig. 6 Elastic moduli (E) of **a, c, e** IPN alginate-CMC beads and **b, d, f** IPN alginate-SEC beads, crosslinked by varying concentrations of Al^{3+} , Fe^{3+} or Cr^{3+} (0.1, 0.2, and 0.5 M)

release kinetics was close to one for IPN alginate-CMC beads (Fig. 7b). But the exponent for alginate beads deviated greatly from unity, which further highlighted the difference in release kinetics between alginate beads and IPN alginate-cellulose beads. The lag time constant, which represents the extent of delayed response, increased with CMC concentrations, as expected, due to the greater crosslinking density of CMC (Fig. 7c). This result demonstrated that the degree of crosslinking of CMC network allowed for the control of the drug release from the IPN alginate-CMC beads.

The release profiles from IPN alginate-SEC beads did not show the sigmoidal pattern, and thus did not

fit well with the Weibull model. They rather fitted well with the Ritger–Peppas model, a power-law dependence on time, suggesting that the drug release was not significantly affected by the secondary SEC network (Fig. 8a) (Hashmi and Dufresne 2009). The kinetic rate constants of IPN alginate-SEC beads were larger than that of alginate beads, despite the presence of the SEC network within the beads (Fig. 8b). This trend is in accordance with the lower rigidity and higher swelling of IPN alginate-SEC beads at higher SEC concentrations, as shown in Figs. 2 and 3.

As a control, drug release profiles from Calcium-alginate-CMC beads were also measured to validate

Fig. 7 **a** Drug release profiles from IPN alginate-CMC beads. The profiles were fitted with the Weibull equation Eq. (3), and **b** the exponent (b), and **c** the lag time (T) were obtained

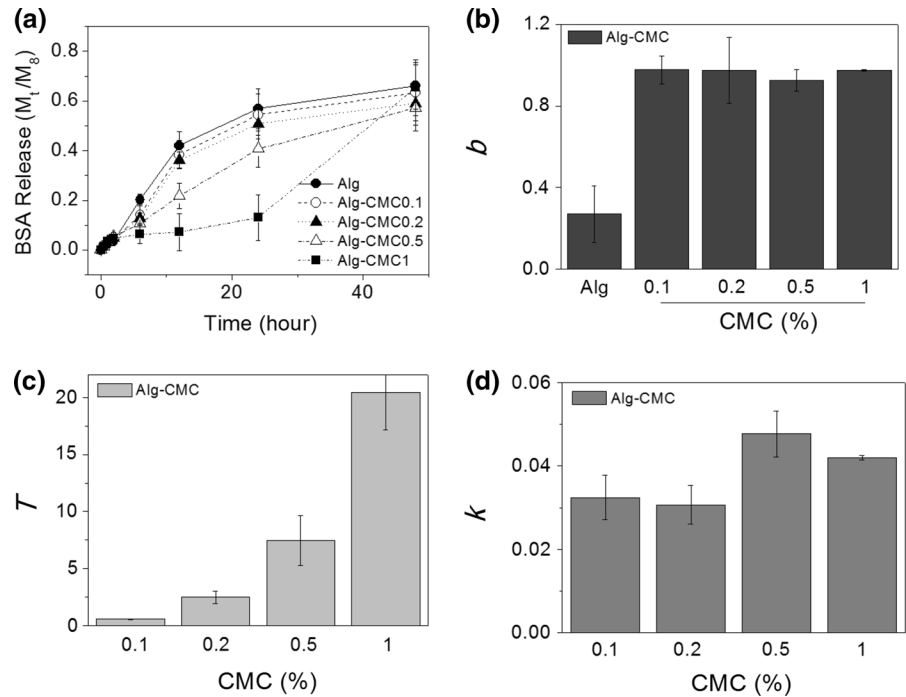
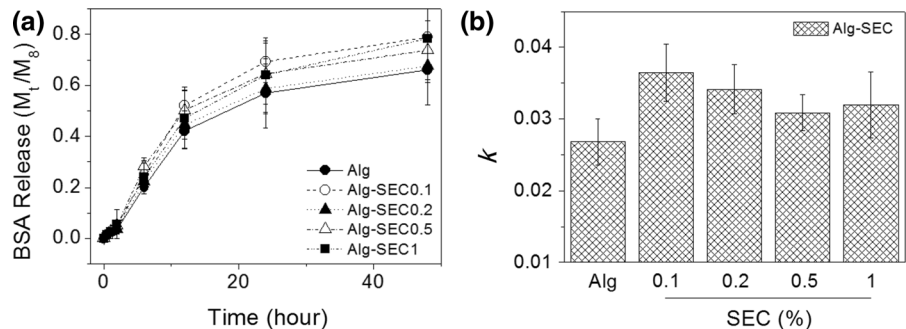


Fig. 8 **a** Drug release profiles from IPN alginate-SEC beads. The profiles were fitted with the Ritger–Peppas equation Eq. (2), and **b** the kinetic rate constants (k) were obtained



the effect of secondary crosslinking of CMC on the release mechanism (Fig. S7 in Supplementary Information). Unlike IPN alginate-CMC beads, the release profiles did not demonstrate the sigmoidal pattern, but rather followed a conventional swelling-controlled Ritger–Peppas model. In addition, the kinetic rate constants increased with CMC concentration, which was opposite to the delayed release from IPN alginate-CMC beads. Similarly, the drug release profiles from Ca-alginate-SEC beads were also measured (Fig. S7 in Supplementary Information). Like the IPN alginate-SEC beads, they fitted well with the Ritger–Peppas model. However, the kinetic rate constants gradually increased with SEC

concentration, similar to those of Ca-alginate-CMC beads. These results highlighted that the presence of non-crosslinked cellulose within the alginate beads helped facilitate the drug release, not acting as a limiting factor, and validated the effect of secondary crosslinking of the cellulose of IPN alginate-cellulose beads on controlling the drug release.

Microbial activity within IPN alginate-cellulose beads

Alginate beads have long been used to immobilize genetically engineered microbial species for sustained and ecofriendly production of industrial

chemicals and fuels. Compared to the raw fermentation method, incorporating bead encapsulation technology provides several benefits. First, it provides protection from harsh processing conditions (e. g. high shear stress, and toxic chemical additives). Second, it allows easy recovery from the fermenting mixture without the need for centrifugation, which is especially attractive for repeated batch fermentation. Third, the efficient mass production of cell-encapsulated beads is possible by simply mixing the cells with the precursor solution. Therefore, *E. coli* capable of producing enhanced green fluorescent protein (GFP⁺-*E. coli*) was used as a model microbial system for encapsulation into the alginate-cellulose beads, and the viability and GFP⁺ expression from the GFP⁺-*E. coli* were evaluated.

For all conditions, the viability of GFP⁺-*E. coli* increased substantially after 1 day of culture, indicating that the cells were able to proliferate within the beads (Fig. 9). For IPN alginate-CMC beads, the

viability at day 1 generally increased with the CMC concentration (Fig. 9a). In addition, the viability was well maintained at the highest CMC concentration (1%) during 3 days of culture, whereas there was a small decrease in viability in other conditions. Similarly for IPN alginate-SEC beads, the viability became larger with SEC concentration at day 1, although the difference was not as significant as that shown for IPN alginate-CMC beads (Fig. 9b). Unlike the IPN alginate-CMC beads, the viability in the IPN alginate-SEC beads at the highest SEC concentration gradually decreased over time and became similar to other conditions. These results suggest that the mechanical properties of the beads had a significant influence over the encapsulated cells; the viability and proliferation were higher in the beads with greater rigidity, and the long term viability was better maintained in the beads with greater structural durability. The effect of enhanced mechanical environment on the encapsulated microbial cells has been

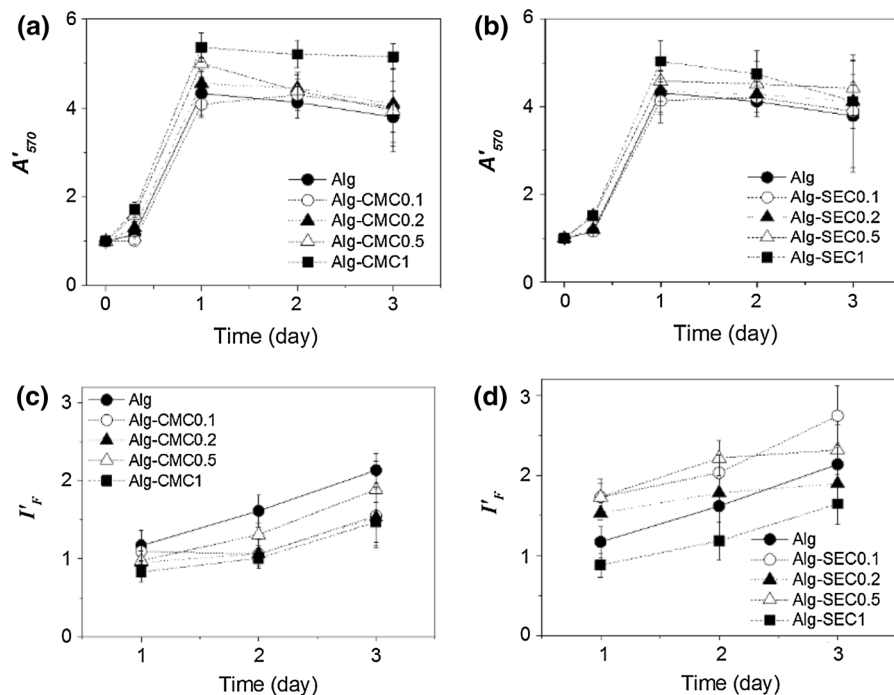


Fig. 9 The normalized viability (A'_{570}) of GFP⁺-*E. coli* encapsulated in (a) IPN alginate-CMC beads and (b) IPN alginate-SEC beads measured over 3 days of culture. The viability at each time point was evaluated by the amount of MTT formazan, metabolized by the living cells, with the characteristic absorbance 570 nm (A_{570}). The values were then normalized with that measured immediately after fabrication

(day 0). The relative fluorescence intensity (I'_F) of the GFP⁺ produced by the encapsulated cells in (c) IPN alginate-CMC beads and (d) IPN alginate-SEC beads. I'_F was calculated by normalizing the fluorescent intensity (I_F) with the viability shown in (a) and (b) to account for the GFP expression by each cell

similarly demonstrated in previous studies (Cha et al. 2012; Chan et al. 2011).

In addition to the viability, the GFP⁺ expression from the encapsulated GFP⁺-*E. coli* was also measured to evaluate the effect of mechanical properties of the beads on the level of gene expression. The adjusted fluorescence intensity (*i.e.* the fluorescence from GFP⁺-*E. coli* normalized with that from wild type *E. coli*, Fig. S8 in Supplementary Information) was normalized with the viability shown in Fig. 9a, b to represent the level of GFP⁺ expression from each living cell in the bead (I'_F). For IPN alginate-CMC beads, I'_F increased over time for all conditions, but the values were lower than that from alginate beads (Fig. 9c). On the other hand, the I'_F from IPN alginate-SEC beads were larger than that from alginate beads, except at the highest SEC concentration (Fig. 9d). These interesting results point to the changes in diffusional properties of the beads having a large impact on the protein expression level; the swelling ratios of IPN alginate-CMC beads were smaller than that of alginate beads, and decreased with CMC concentration, whereas the swelling ratios of IPN alginate-SEC beads increased with SEC concentration (Fig. 3). The diffusional limit caused by the increased crosslinking density of the beads likely diminished the metabolic rate by the encapsulated cells. At any rate, the protein expression from the encapsulated GFP⁺-*E. coli* increased over time for all bead conditions, demonstrating their biocompatibility and utility as a cell-encapsulating vehicle.

Conclusion

Taken together, this study demonstrated a comprehensive examination of interpenetrating network (IPN) of alginate-cellulose beads prepared by a dual ionic crosslinking method. Aqueous-soluble anionic celluloses, carboxymethyl cellulose (CMC) and sulfoethyl cellulose (SEC), were capable of undergoing ionic crosslinking reaction with multivalent cations. Interestingly, they were more dominantly crosslinked by trivalent cations (e.g. Al³⁺, Cr³⁺ and Fe³⁺) than divalent Ca²⁺. This aspect necessitated the need for the sequential crosslinking strategy to engineer the IPN alginate-cellulose beads; alginate crosslinking by divalent ions followed by cellulose crosslinking by trivalent ions. Mechanical and diffusional properties

of the IPN alginate-cellulose beads could be controlled in a wide range by the concentrations of cellulose and crosslinking trivalent ions. The structural durability of the beads against a chelating environment was also enhanced by the IPN formation. These controllable properties of the IPN alginate-cellulose beads allowed for their utilization as carriers of biological entities, as demonstrated by the ability to control the drug release rate and the activity of encapsulated microbial cells. It is expected that the strategy of creating IPN via dual ionic crosslinking in an efficient and controllable manner as presented in this study could be utilized in various forms of materials for biomedical applications.

Acknowledgments This study was supported by the 2017 Research Fund (1.170008.01 and 1.170050.01) of UNIST (Ulsan National Institute of Science and Technology) and Civil-Military Technology Cooperation Program (15-CM-SS) of Korea.

References

- Agarwal T, Narayana SNGH, Pal K, Pramanik K, Giri S, Banerjee I (2015) Calcium alginate-carboxymethyl cellulose beads for colon-targeted drug delivery. *Int J Biol Macromol* 75:409–417. doi:[10.1016/j.ijbiomac.2014.12.052](https://doi.org/10.1016/j.ijbiomac.2014.12.052)
- Anseth KS, Bowman CN, Brannon-Peppas L (1996) Mechanical properties of hydrogels and their experimental determination. *Biomaterials* 17:1647–1657. doi:[10.1016/0142-9612\(96\)87644-7](https://doi.org/10.1016/0142-9612(96)87644-7)
- Bashan Y (1986) Alginate beads as synthetic inoculant carriers for slow release of bacteria that affect plant growth. *Appl Environ Microbiol* 51:1089–1098
- Cha C, Kim SR, Jin Y-S, Kong H (2012) Tuning structural durability of yeast-encapsulating alginate gel beads with interpenetrating networks for sustained bioethanol production. *Biotechnol Bioeng* 109:63–73. doi:[10.1002/bit.23258](https://doi.org/10.1002/bit.23258)
- Cha C et al (2014) Microfluidics-assisted fabrication of gelatin-silica core-shell microgels for injectable tissue constructs. *Biomacromol* 15:283–290. doi:[10.1021/bm401533y](https://doi.org/10.1021/bm401533y)
- Chan ES et al (2011) Effects of starch filler on the physical properties of lyophilized calcium-alginate beads and the viability of encapsulated cells. *Carbohydr Polym* 83:225–232. doi:[10.1016/j.carbpol.2010.07.044](https://doi.org/10.1016/j.carbpol.2010.07.044)
- Chitprasert P, Sudsai P, Rodklongtan A (2012) Aluminum carboxymethyl cellulose-rice bran microcapsules: Enhancing survival of *Lactobacillus reuteri* KUB-AC5. *Carbohydr Polym* 90:78–86. doi:[10.1016/j.carbpol.2012.04.065](https://doi.org/10.1016/j.carbpol.2012.04.065)
- Chremos A, Douglas JF (2016) Influence of higher valent ions on flexible polyelectrolyte stiffness and counter-ion distribution. *J Chem Phys* 144:164904. doi:[10.1063/1.4947221](https://doi.org/10.1063/1.4947221)

- Cormack BP, Valdivia RH, Falkow S (1996) FACS-optimized mutants of the green fluorescent protein (GFP). *Gene* 173:33–38. doi:[10.1016/0378-1119\(95\)00685-0](https://doi.org/10.1016/0378-1119(95)00685-0)
- Covarrubias SA, de Bashan LE, Moreno M, Bashan Y (2012) Alginate beads provide a beneficial physical barrier against native microorganisms in wastewater treated with immobilized bacteria and microalgae. *Appl Microbiol Biotechnol* 93:2669–2680. doi:[10.1007/s00253-011-3585-8](https://doi.org/10.1007/s00253-011-3585-8)
- Dash S, Murthy PN, Nath L, Chowdhury P (2010) Kinetic modeling on drug release from controlled drug delivery systems. *Acta Pol Pharm* 67:217–223
- Emregül E, Sungur S, Akbulut U (1996) Effect of chromium salts on invertase immobilization onto carboxymethyl-cellulose-gelatine carrier system. *Biomaterials* 17:1423–1427. doi:[10.1016/0142-9612\(96\)87285-1](https://doi.org/10.1016/0142-9612(96)87285-1)
- Fan L, Zhang J, Wang A (2013) In situ generation of sodium alginate/hydroxyapatite/halloysite nanotubes nanocomposite hydrogel beads as drug-controlled release matrices. *J Mater Chem B* 1:6261–6270. doi:[10.1039/C3TB20971G](https://doi.org/10.1039/C3TB20971G)
- Fang A, Cathala B (2011) Smart swelling biopolymer microparticles by a microfluidic approach: synthesis, in situ encapsulation and controlled release. *Colloids Surf B Biointerfaces* 82:81–86. doi:[10.1016/j.colsurfb.2010.08.020](https://doi.org/10.1016/j.colsurfb.2010.08.020)
- Fu Y, Kao WJ (2009) Drug release kinetics and transport mechanisms from semi-interpenetrating networks of gelatin and poly(ethylene glycol) diacrylate. *Pharm Res*. doi:[10.1007/s11095-009-9923-1](https://doi.org/10.1007/s11095-009-9923-1)
- George M, Abraham TE (2006) Polyionic hydrocolloids for the intestinal delivery of protein drugs: alginate and chitosan—a review. *J Control Release* 114:1–14. doi:[10.1016/j.jconrel.2006.04.017](https://doi.org/10.1016/j.jconrel.2006.04.017)
- Gombotz WR, Wee SF (2012) Protein release from alginate matrices *Adv Drug Deliver Rev* 64(Supplement):194–205. doi:[10.1016/j.addr.2012.09.007](https://doi.org/10.1016/j.addr.2012.09.007)
- Hari PR, Chandu T, Sharma CP (1996) Chitosan/calcium–alginate beads for oral delivery of insulin. *J Appl Polym Sci* 59:1795–1801
- Hashmi SM, Dufresne ER (2009) Mechanical properties of individual microgel particles through the deswelling transition. *Soft Matter* 5:3682–3688. doi:[10.1039/B906051K](https://doi.org/10.1039/B906051K)
- Hoenich N (2006) Cellulose for medical applications: past, present, and future. *BioRes* 1:270–280
- Jang J, Hong J, Cha C (2017) Effects of precursor composition and mode of crosslinking on mechanical properties of graphene oxide reinforced composite hydrogels. *J Mech Behav Biomed Mater* 69:282–293. doi:[10.1016/j.jmbbm.2017.01.025](https://doi.org/10.1016/j.jmbbm.2017.01.025)
- Jorfi M, Foster EJ (2015) Recent advances in nanocellulose for biomedical applications. *J Appl Polym Sci*. doi:[10.1002/app.41719](https://doi.org/10.1002/app.41719)
- Kil KC, Paik U (2015) Lithium salt of carboxymethyl cellulose as an aqueous binder for thick graphite electrode in lithium ion batteries. *Macromol Res* 23:719–725. doi:[10.1007/s13233-015-3094-1](https://doi.org/10.1007/s13233-015-3094-1)
- Kim MS, Park SJ, Gu BK, Kim C-H (2012) Ionically cross-linked alginate–carboxymethyl cellulose beads for the delivery of protein therapeutics. *Appl Surf Sci* 262:28–33. doi:[10.1016/j.apsusc.2012.01.010](https://doi.org/10.1016/j.apsusc.2012.01.010)
- Kim S, Lee K, Cha C (2016) Refined control of thermoresponsive swelling/deswelling and drug release properties of poly(*N*-isopropylacrylamide) hydrogels using hydrophilic polymer crosslinkers. *J Biomater Sci Polym Ed* 27:1698–1711. doi:[10.1080/09205063.2016.1230933](https://doi.org/10.1080/09205063.2016.1230933)
- Ko H-U, John A, Mun S, Im J, Kim J (2015) Preparation and characterization of Cellulose-ZnO nanolayer film by blending method. *Macromol Res* 23:814–818. doi:[10.1007/s13233-015-3111-4](https://doi.org/10.1007/s13233-015-3111-4)
- Kulkarni AR, Soppimath KS, Aminabhavi TM, Rudzinski WE (2001) In-vitro release kinetics of cefadroxil-loaded sodium alginate interpenetrating network beads. *Eur J Pharm Biopharm* 51:127–133. doi:[10.1016/S0939-6411\(00\)00150-8](https://doi.org/10.1016/S0939-6411(00)00150-8)
- Lee KY, Mooney DJ (2012) Alginate: properties and biomedical applications. *Prog Polym Sci* 37:106–126. doi:[10.1016/j.progpolymsci.2011.06.003](https://doi.org/10.1016/j.progpolymsci.2011.06.003)
- Lee TS et al (2011) BglBrick vectors and datasheets: a synthetic biology platform for gene expression. *J Biol Eng* 5:12. doi:[10.1186/1754-1611-5-12](https://doi.org/10.1186/1754-1611-5-12)
- Lee JY, Kwak HW, Yun H, Kim YW, Lee KH (2016) Methyl cellulose nanofibrous mat for lipase immobilization via cross-linked enzyme aggregates. *Macromol Res* 24:218–225. doi:[10.1007/s13233-016-4028-2](https://doi.org/10.1007/s13233-016-4028-2)
- Lim F, Sun AM (1980) Microencapsulated islets as bioartificial endocrine pancreas *Science* 210:908–910. doi:[10.1126/science.6776628](https://doi.org/10.1126/science.6776628)
- Lin DC, Dimitriadis EK, Horkay F (2007) Elasticity of rubber-like materials measured by AFM nanoindentation *Express Polym Lett* 1:576–584. doi:[10.3144/expresspolymlett.2007.79](https://doi.org/10.3144/expresspolymlett.2007.79)
- Mørch YÁ, Donati I, Strand BL (2006) Effect of Ca²⁺, Ba²⁺, and Sr²⁺ on alginate microbeads. *Biomacromol* 7:1471–1480. doi:[10.1021/bm060010d](https://doi.org/10.1021/bm060010d)
- Ouwercx C, Velings N, Mestdagh MM, Axelos MAV (1998) Physico-chemical properties and rheology of alginate gel beads formed with various divalent cations *Polym Gels Networks* 6:393–408. doi:[10.1016/S0966-7822\(98\)00035-5](https://doi.org/10.1016/S0966-7822(98)00035-5)
- Pfister G, Bahadir M, Korte F (1986) Release characteristics of herbicides from Ca alginate gel formulations. *J Control Release* 3:229–233. doi:[10.1016/0168-3659\(86\)90094-5](https://doi.org/10.1016/0168-3659(86)90094-5)
- Ramos LA, Frollini E, Heinze T (2005) Carboxymethylation of cellulose in the new solvent dimethyl sulfoxide/tetrabutylammonium fluoride. *Carbohydrate Polym* 60:259–267. doi:[10.1016/j.carbpol.2005.01.010](https://doi.org/10.1016/j.carbpol.2005.01.010)
- Rathore S, Desai PM, Liew CV, Chan LW, Heng PWS (2013) Microencapsulation of microbial cells. *J Food Eng* 116:369–381. doi:[10.1016/j.jfoodeng.2012.12.022](https://doi.org/10.1016/j.jfoodeng.2012.12.022)
- Serra L, Doménech J, Peppas NA (2006) Drug transport mechanisms and release kinetics from molecularly designed poly(acrylic acid-g-ethylene glycol) hydrogels. *Biomaterials* 27:5440–5451. doi:[10.1016/j.biomaterials.2006.06.011](https://doi.org/10.1016/j.biomaterials.2006.06.011)
- Shen Y et al (2016) pH and redox dual stimuli-responsive injectable hydrogels based on carboxymethyl cellulose derivatives. *Macromol Res* 24:602–608. doi:[10.1007/s13233-016-4077-6](https://doi.org/10.1007/s13233-016-4077-6)
- Shi J, Alves NM, Mano JF (2008) Chitosan coated alginate beads containing poly(*N*-isopropylacrylamide) for dual-stimuli-responsive drug release. *J Biomed Mater Res Part*

- B: *Appl Biomater* 84B:595–603. doi:[10.1002/jbm.b.30907](https://doi.org/10.1002/jbm.b.30907)
- Sindhu KA, Prasanth R, Thakur VK (2014) Medical applications of cellulose and its derivatives: present and future. In: *Nanocellulose Polymer Nanocomposites*. John Wiley and Sons, Inc., pp 437–477. doi:[10.1002/9781118872246.ch16](https://doi.org/10.1002/9781118872246.ch16)
- Siritientong T, Aramwit P (2015) Characteristics of carboxymethyl cellulose/sericin hydrogels and the influence of molecular weight of carboxymethyl cellulose. *Macromol Res* 23:861–866. doi:[10.1007/s13233-015-3116-z](https://doi.org/10.1007/s13233-015-3116-z)
- Smidsrød O, Skjåk-Bræk G (1990) Alginate as immobilization matrix for cells. *Trends Biotechnol* 8:71–78. doi:[10.1016/0167-7799\(90\)90139-O](https://doi.org/10.1016/0167-7799(90)90139-O)
- Sugiura S et al (2005) Size control of calcium alginate beads containing living cells using micro-nozzle array. *Biomaterials* 26:3327–3331. doi:[10.1016/j.biomaterials.2004.08.029](https://doi.org/10.1016/j.biomaterials.2004.08.029)
- Thu B, Bruheim P, Espevik T, Smidsrød O, Soon-Shiong P, Skjåk-Bræk G (1996a) Alginate polycation microcapsules: I. interaction between alginate and polycation. *Biomaterials* 17:1031–1040. doi:[10.1016/0142-9612\(96\)84680-1](https://doi.org/10.1016/0142-9612(96)84680-1)
- Thu B, Bruheim P, Espevik T, Smidsrød O, Soon-Shiong P, Skjåk-Bræk G (1996b) Alginate polycation microcapsules: II. some functional properties. *Biomaterials* 17:1069–1079. doi:[10.1016/0142-9612\(96\)85907-2](https://doi.org/10.1016/0142-9612(96)85907-2)
- Tønnesen HH, Karlsen J (2002) Alginate in drug delivery systems. *Drug Dev Ind Pharm* 28:621–630. doi:[10.1081/DDC-120003853](https://doi.org/10.1081/DDC-120003853)
- Van Benschoten JE, Edzwald JK (1990) Chemical aspects of coagulation using aluminum salts—I. hydrolytic reactions of alum and polyaluminum chloride. *Water Res* 24:1519–1526. doi:[10.1016/0043-1354\(90\)90086-L](https://doi.org/10.1016/0043-1354(90)90086-L)
- Xiao C, Li H, Gao Y (2009) Preparation of fast pH-responsive ferric carboxymethylcellulose/poly(vinyl alcohol) double-network microparticles. *Polym Int* 58:112–115. doi:[10.1002/pi.2502](https://doi.org/10.1002/pi.2502)
- Xiong G, Luo H, Zhang C, Zhu Y, Wan Y (2015) Enhanced biological behavior of bacterial cellulose scaffold by creation of macropores and surface immobilization of collagen. *Macromol Res* 23:734–740. doi:[10.1007/s13233-015-3099-9](https://doi.org/10.1007/s13233-015-3099-9)
- Yang XH, Zhu WL (2007) Viscosity properties of sodium carboxymethylcellulose solutions *Cellulose* 14:409–417. doi:[10.1007/s10570-007-9137-9](https://doi.org/10.1007/s10570-007-9137-9)
- Zhang L-M (2001) New water-soluble cellulosic polymers: a review. *Macromol Mater Eng* 286:267–275. doi:[10.1002/1439-2054\(20010501\)286:5<267:AID-MAME267>3.0.CO;2-3](https://doi.org/10.1002/1439-2054(20010501)286:5<267:AID-MAME267>3.0.CO;2-3)
- Zhang J, Wang Q, Wang A (2010) In situ generation of sodium alginate/hydroxyapatite nanocomposite beads as drug-controlled release matrices. *Acta Biomater* 6:445–454. doi:[10.1016/j.actbio.2009.07.001](https://doi.org/10.1016/j.actbio.2009.07.001)
- Zhang K, Brendler E, Gebauer K, Gruner M, Fischer S (2011) Synthesis and characterization of low sulfoethylated cellulose *Carbohydrate Polym* 83:616–622. doi:[10.1016/j.carbpol.2010.08.030](https://doi.org/10.1016/j.carbpol.2010.08.030)